Earth System Changes in Marginal Seas/Oceanologia 65 (2023) 71—85

Available online at www.sciencedirect.com

ScienceDirect

journal homepage: www.journals.elsevier.com/oceanologia

ORIGINAL RESEARCH ARTICLE

Nearshore sandbar switching episodes and their relationship with coastal erosion at the Curonian Spit, Baltic Sea

Rasa Janušaitė[a,*], Darius Jarmalavičius[a], Donatas Pupienis[a], Gintautas Žilinskas[a], Laurynas Jukna[b]

[a] *Laboratory of Geoenvironmental Research, Nature Research Centre, Vilnius, Lithuania*
[b] *Institute of Geosciences, Vilnius University, Vilnius, Lithuania*

Received 30 August 2021; accepted 22 November 2021
Available online 5 December 2021

KEYWORDS
Nearshore morphodynamics;
Multiple sandbar system;
Storms;
Sand volume;
Lithuania

Abstract The longshore realignment of nearshore sandbars is a morphodynamic phenomenon of multiple sandbar systems that has been known about for several decades. However, it is unknown how switching-related nearshore changes influence the evolution of subaerial beaches. This study aims to define the relationship between sandbar switching episodes and the dynamic state of the beach-foredune system along the Curonian Spit coast (Baltic Sea) using decadal satellite-derived and beach profiling data. To define this connection, sandbar switching locations, sandbar cross-shore positions, shoreline positions, and sand volume changes in the beach-foredune system were assessed on interannual and storm-related time scales. Twenty-seven sandbar switching episodes were observed with an average duration of 14.3 months. Most of the switching episodes occurred at preferred locations, coinciding with breaking points of different shoreline orientations where oblique waves and longshore currents prevailed. Shoreline retreat at an average rate of −14.2 m was observed within most of the sandbar switching zones. During major storm events, the average rate of erosion within the sandbar switching zones was significantly higher than the rate outside them. On an interannual time scale, a moderate average rate of erosion was observed within the sandbar switching zones compared to a small accretion rate outside them. Additional case studies of coastal evolution within the

* Corresponding author at: Laboratory of Geoenvironmental Research, Nature Research Centre, Akademijos Str. 2, 08412, Vilnius, Lithuania.
E-mail address: rasa.janusaite@gamtc.lt (R. Janušaitė).
Peer review under the responsibility of the Institute of Oceanology of the Polish Academy of Sciences.

ELSEVIER Production and hosting by Elsevier

https://doi.org/10.1016/j.oceano.2021.11.004
0078-3234/

switching zones indicated well-correlated rates of switching-determined outer sandbar positions, shoreline positions, and sand volume on the beach and foredune during the switching episodes. The results of this study could be important for the identification of erosional hot spots and coastal prediction.

1. Introduction

The magnitude and occurrence of coastal erosion are spatiotemporally variable and controlled by complex natural and anthropogenic factors (Stive et al., 2002). In sandy environments, natural factors include wave climate, sea-level fluctuations, coastal orientation, and antecedent or nearshore morphology (Del Río et al., 2013; Stive et al., 2002). The key feature characterising the latter is nearshore sandbars. Various studies have aimed to determine links between the dynamics of nearshore sandbars and subaerial beaches on a range of temporal scales: from long-term and middle-term (Aagaard et al., 2004; McNinch, 2004; Splinter et al., 2018; Stive et al., 1997; Tătui et al., 2013; Umeda et al., 2018; Yuhi and Umeda, 2018), to short-term and storm-related (Castelle et al., 2015, 2007; Kuznetsova and Saprykina, 2019). They related the short-term and mid-term variability of shoreline and sediment volume on subaerial beaches to the cyclic variability of sandbar systems during net offshore migration (NOM) (Parlagreco et al., 2019; Shand et al., 2006; Yuhi et al., 2016; Yuhi and Umeda, 2018); observed beach sediment supply from sandbar welding (Aagaard et al., 2004; Cohn et al., 2017) and coupled shoreline and sandbar behaviour (Balouin et al., 2013; Gijsman et al., 2021; Pruszak et al., 2008; Quartel et al., 2008; Ruessink et al., 2007; Van de Lageweg et al., 2013); documented the role of nearshore sandbars in the formation of coastal erosion spots during storm events (Castelle et al., 2019, 2015, 2007; Harley et al., 2009; Thornton et al., 2007) and post-storm shoreline recovery (Brooks et al., 2017; Phillips et al., 2017). Although a considerable amount of research has been devoted to understanding connections between subaerial beaches and subaqueous sandbars, there are still many unknowns about these interactions.

At the end of the last century sandbar switching as a feature of multiple sandbar system behaviour was observed (Shand and Bailey, 1999; Wijnberg and Wolf, 1994). It involves longshore sandbars becoming discontinuous and on their discontinuous side attaching to a landward or seaward sandbar (Shand, 2003; Shand et al., 2001). A sandbar switching period consisting of interrelated sandbar switches is referred to as a sandbar switching episode (Shand et al., 2001). The longshore area of a sandbar switching episode extends from several hundred meters to a few kilometres, and is referred to as a transitional zone (Aleman et al., 2017; Shand et al., 2001; Wijnberg and Wolf, 1994) or, in this study, a sandbar switching zone.

Sandbar realignment has been observed in video observations, bathymetric datasets, aerial photography, and LiDAR data on microtidal and mesotidal coasts (Aleman et al., 2017; Bouvier et al., 2017; Ojeda et al., 2008; Shand, 2003; Shand et al., 2001; Walstra et al., 2016; Wijnberg et al., 2007; Wijnberg and Wolf, 1994). The current knowledge about sandbar switching episodes can be summarised as follows: 1) naturally, they seem to be caused by shore-oblique high energy events and strong longshore currents if longshore differences in the sandbar morphology are present (Aleman et al., 2017; Shand et al., 2001); 2) they may be triggered by alongshore variability related to shoreface nourishment or underwater coastal engineering structures (Bouvier et al., 2017; Ojeda et al., 2008; Vermaas et al., 2017; Wijnberg et al., 2007); 3) sandbar switching locations may be persistent or non-persistent (Walstra et al., 2016); 4) persistent switching locations are transitional zones between multiple sandbar systems exhibiting different characteristics of the NOM cycle (Walstra et al., 2016); 5) sandbar switching zones migrate alongshore at a rate of between tens and hundreds of meters per month (Shand et al., 2001; Wijnberg and Wolf, 1994); 6) sandbar switches may be shoreward propagating (migrating from outer-middle sandbar switches to middle-inner ones) or stationary (Shand et al., 2001); 7) sandbar switching is not a seasonal phenomenon and its effect on nearshore morphodynamic system lasts for several seasons (Wijnberg et al., 2007). A sandbar switching episode is associated with significant changes in sandbar cross-shore and longshore positions, which affects the nearshore flow field and may cause changes in coastal evolution. However, interactions between these transitional zones in the subaqueous and subaerial domains have never been studied to the best of our knowledge.

In this study, sandbar switching is explored as being one of the factors determining interannual and storm-induced coastal erosion. The primary aim of this study is to define the relationship between sandbar switching episodes and the evolution of subaerial beaches in a non-tidal wave-dominated environment on the Lithuanian part of the Curonian Spit coast (South-Eastern Baltic Sea). To achieve this, the occurrence and persistence of sandbar switching on the Curonian Spit are determined. Satellite-derived shoreline changes in the coastal areas of sandbar switching are assessed and the relationship between sandbar switching and sand volume on a subaerial beach is defined on interannual and storm-related time scales.

2. Material and methods

2.1. Study area

The Curonian Spit is a sandy barrier in the South-Eastern Baltic Sea, stretching for 98 km from the Sambia Peninsula

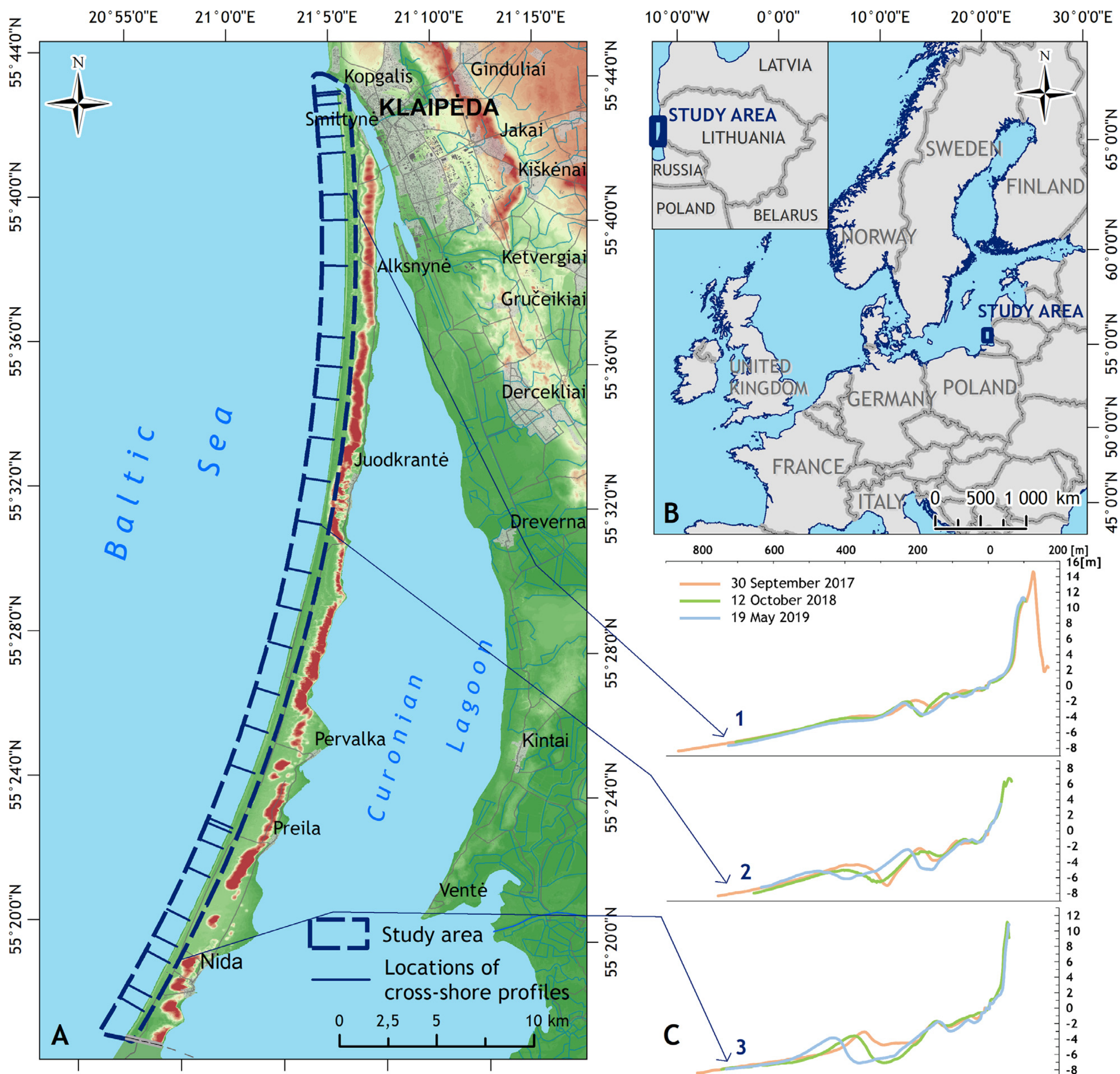

Figure 1 The study area in the Lithuanian part of the Curonian Spit configuration with the locations of the topographic surveys (A), the location of the study area (B), and examples of coastal cross-shore profiles (C).

to the Klaipėda Strait. The 51 km-long northern part of the Curonian Spit, from the Klaipėda port jetty to the Lithuanian state border, was analysed in this study (Figure 1). The Curonian Spit coast is a non-tidal wave-dominated environment. Waves approaching from westerly directions (North-West, South-West, West) are dominant on the nearshore of the Curonian Spit. The annual mean wave height at Klaipėda is 0.5—1 m (Kelpšaitė and Dailidienė, 2011). The wave climate on the nearshore of the Curonian Spit is seasonal, with a mean wave height of 0.76 and 0.85 m in winter and autumn, and 0.56 and 0.62 m in spring and summer (Jakimavičius et al., 2018). The morphology of the study area mostly results from natural coastal evolution, but the development of the northern end of the Curonian Spit is influenced by the Klaipėda port jetty (Žilinskas et al., 2020).

The subaerial section of the Curonian Spit coast is characterised by sandy beaches, composed of fine and medium sand, and bordered by a foredune ridge. The beaches are 30—80 m wide and the foredune height ranges from 6 to 16 m (Figure 1c) (Jarmalavičius et al., 2017; Žilinskas et al., 2018). The underwater slope of the Curonian Spit consists of a multiple sandbar system with 2—5 longshore sandbars. The width of the sandbar zone from the shoreline to the lower limit of the seaward outer sandbar slope varies from 250 to 750 m. The nearshore slope (tan β) in the sandbar zone is 0.009—0.014. The northern part of the study area is characterised by the smallest sandbars, and the lowest sandbar zone width, slope, and depth (Figure 1c). The southern part of the study area is characterised by the largest sandbars, a wider sandbar zone, a higher nearshore slope, and a greater depth (Figure 1c). The multiple sandbar system on the nearshore of the Curonian Spit exhibits various types of morphologies, from longshore straight to crescentic (mostly irregular) and shore-attached.

2.2. Field and satellite data

In this study, a combination of multispectral satellite imagery and cross-section beach profiling surveys for the period 2009—2021 was used to assess morphological changes in the nearshore and subaerial beach.

The beach profiling was performed at 30 fixed cross-shore profiles (Figure 1a) every April—May using the Topcon HiPer SR Global Navigation Satellite System (GNSS) with a vertical accuracy of 0.015 m. The beach profiling data were used to evaluate interannual sand volume changes on the beach and foredune. Surveys to evaluate storm-induced sand volume changes were carried out within a week after a storm event when the weather had calmed down and the water level had dropped.

42 RapidEye (for the period 2009—2016) and 103 PlanetScope (for the period 2016—2021) images were employed for the shoreline extraction and identification of the sandbar switching phenomenon. RapidEye is a constellation of five identical push-broom satellite sensors that acquired five-band (Blue, Green, Red, Red-Edge, Near-Infrared) imagery with a spatial resolution of 5 m every 5.5 days during the period 2009—2020. PlanetScope is a constellation of approximately 130 satellites that has acquired four-band (Blue, Green, Red, Near-Infrared) imagery daily with a spatial resolution of 3 m since 2016. In this study, atmospherically and geometrically corrected (to $<$10 m RMSE positional accuracy) RapidEye Level 3A and PlanetScope Level 3B products were used (Planet, 2021; Planet Team, 2017).

To identify sandbar switching locations during major storm events that occurred before the launch of the RapidEye constellation, imagery of Landsat-4 and Landsat-5 Thematic Mapper (TM) was used. The Landsat 4—5 TMs are multispectral satellite sensors that collected seven-band (spectral range 450—1250 nm) imagery with a spatial resolution of 30 m and a temporal resolution of 16 days during the period 1982—2012. Landsat Level-2 surface reflectance products were used in this study (USGS, 1998).

The presence of sandbar switching during storm events was identified using satellite images from the last and first available dates when the sandbar morphology was clearly visible before and after the storm events. The time between the storm and image acquisition date ranged from 4 to 11 days for storm Laura and from 45 to 75 days for storm Felix. Because the average duration of a sandbar switching episode on the Curonian Spit is 435 days, sandbar switching was considered to be present during a storm event if it was observed before and after the storm.

2.3. Identification and definition of sandbar switching zones

Every satellite image for the period 2009—2021 was inspected visually and sandbar switching zones were localised manually. Sandbar switching zone was defined as a nearshore area stretching in an alongshore direction 500 m to the north and 500 m to the south of the point where the sandbar joined another seaward or landward-located sandbar (Figure 2a). If switching occurred between multiple sandbars, a distance of 500 m was calculated from the northernmost and southernmost joins (Figure 2b). The defined sandbar switching zone covered the area where the morphology of the sandbar system was affected by the switching. The first observation, last observation, duration, position of the switched sandbars, and switching type were fixed for each switching zone. The image acquisition date, when a sandbar was observed to be connected to another sandbar for the first time was considered to be the first observation; the image acquisition date when a sandbar join was visible for the last time was considered to be last observation. Switches involving outer and middle sandbars were analysed in this study; switches involving inner sandbars only were ignored due to the complexity of the inner nearshore morphology and their small influence on the characteristics of the overall sandbar system. The position of the outer sandbar was assessed to be the distance of the outer sandbar crest from the mean shoreline. Changes in the distance of the outer sandbar from the mean shoreline was considered to be one of the characteristics that showed switching-induced changes in the sandbar system. Sandbar crests were delineated from the PlanetScope and RapidEye images using an automated procedure, described in Janušaitė et al. (2021), with an average root mean square error (*RMSE*) of 5.8 and 7 m, respectively.

2.4. Determination of subaerial beach characteristics

An automated algorithm was designed for the shoreline extraction from the satellite images used in this study. The Normalized Difference Water Index (NDWI) (McFeeters, 1996) was calculated for the images and was used as input for the ISODATA unsupervised classification in combination with a near-infrared band to classify the images into land or sea (for the detailed procedure see Janušaitė et al., 2021). The boundary between land and sea was considered to be shoreline. Using this method, the shorelines were derived with an average *RMSE* of 4.4 m.

Shoreline-perpendicular transects were generated along the study area every 25 meters to evaluate changes in the shoreline position. The shoreline position, fixed one year before the first observation of a sandbar switching episode, was used as a starting point to calculate the shoreline change rate for a specific date. Every procedure involving satellite images was performed in the ArcGIS 10.7 environment.

The annual sand volume changes were calculated for the beach and foredune from the cross-shore profiles by comparing two successive years. To evaluate the impact of storms, the last cross-shore profiles before a storm were compared to those, measured after the storm. The sand volume in the cross-shore profiles was defined as an area enclosed by the beach and foredune surface and a horizontal line from the shoreline to the foredune landward toe. The mean of the annual and post-storm sand volume change rate in the profiles inside and outside the sandbar switching zones was compared using a two-sample t-test and the me-

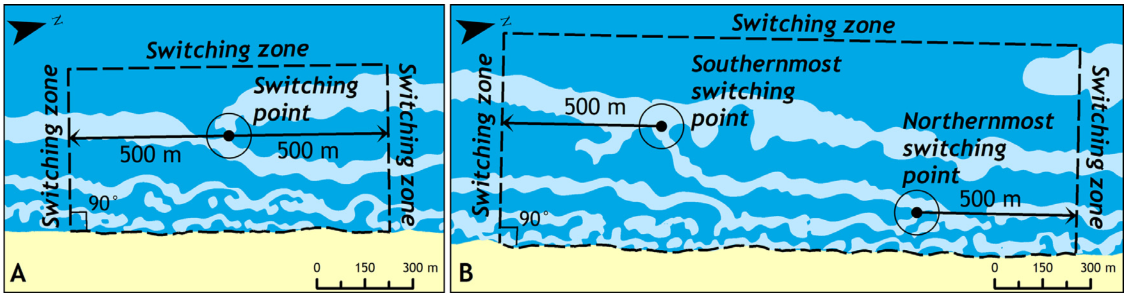

Figure 2 Definition of sandbar switching zone boundaries: A — a case of a switching zone with a single switch within its boundaries; B — a case of a switching zone with multiple switches within its boundaries.

Table 1 Duration of sandbar switching episodes on the Curonian Spit.

Type of switching episode	Number of observations	Duration of switching episode [months]				
		Average	Median	25—75%	Min	Max
Permanent switch	12	18.0	13	8.0—25.5	2	49
Temporary switch	11	9.3	6	5.0—15.0	2	26
Temporary connection	4	17.3	12	8.8—31.0	8	37
Total	**27**	**14.3**	**11**	**6—18**	**2**	**49**

dian of the annual and post-storm sand volume change rate was compared using an unpaired two-sample Wilcoxon test.

3. Results

3.1. Sandbar switching zones

3.1.1. Temporal and morphological characteristics

For the period 2009—2021, 27 sandbar switching episodes were observed on the Curonian Spit with an average duration of 14.3 months (Table 1). The majority of these sandbar switching episodes appeared after a stormy winter season and lasted for at least one season until the next winter. 14 switching episodes occurred between the outer and middle sandbars (outer-middle sandbar switch), 1 between the outer and inner (outer-inner sandbar switch), and 12 between multiple sandbars (outer-middle, middle-inner sandbar switch).

Three types of sandbar switching were observed: permanent switch, temporary switch, and temporary connection (Figure 3). A permanent switch is defined as a switch that occurs when a sandbar joins another seaward or landward located sandbar, takes its position, and continues to develop in that position (Figure 3a). A temporary switch is when a sandbar takes the place of another sandbar, but after some time returns to its primary position (Figure 3b). A temporary connection is when a sandbar joins another landward or seaward-located sandbar but switching does not occur (Figure 3c). Permanent and temporary switches were the most common types during the analysed period (Table 1).

3.1.2. Spatial characteristics

Between 2009 and 2021, the switching zones were distributed unevenly along the Curonian Spit (Figure 4). After completion, the switching episodes reoccurred in the same or a close-by location. This property allows approximate stretches to be distinguished where sandbar switching is typically absent and present along the Curonian Spit nearshore: no switching episodes were typically observed in the northern section of the study area; the northernmost switching zone was observed to the south of Alksnynė (13.5—14.5 km from the Klaipėda port jetty); the second was observed to the south of Juodkrantė (21 km from the Klaipėda port jetty); the third was observed in the area between 26 and 28 km from the Klaipėda port jetty; the fourth was observed to the north or south of Pervalka (32—36 km from the Klaipėda port jetty), the fifth was observed at Preila (38.5 km from the Klaipėda port jetty); the sixth was observed to the north of Nida (42.5—43.5 km from the Klaipėda port jetty); the seventh was observed in the southern part of Nida (47.5 km from the Klaipėda port jetty) (Figure 4). Switching episodes also occurred in other locations, but they were not spatially recurrent. Figure 4a shows that the majority of the recurrent sandbar switching locations on the Curonian Spit were observed in locations where the orientation of the mean shoreline for the period 2009—2021 was changing.

3.2. Shoreline changes in the sandbar switching zones

Shoreline retreat at an average rate of −14.2 m occurred in 25 (out of 27) sandbar switching zones, which were observed during the period 2009—2021. The average length of the shoreline retreat area in the switching zones was 554.6 m and the average area of the shoreline retreat was 12.8 m^2/m. Figure 5 shows the shoreline change characteristics in different sandbar switching zones on the dates of maximum shoreline retreat.

Several scenarios of shoreline behaviour were observed in the sandbar switching zones:

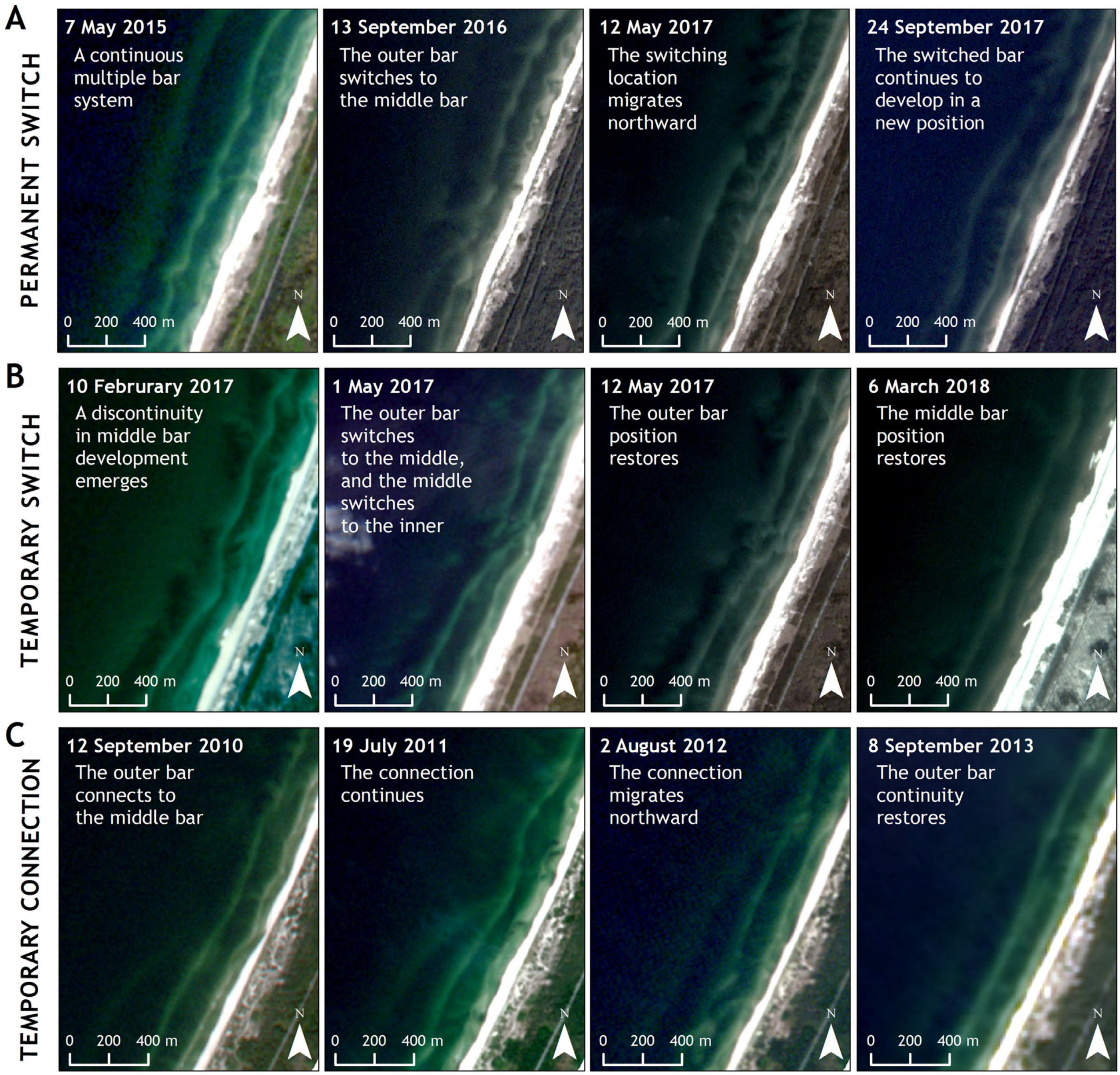

Figure 3 Examples of three different sandbar switching types on the Curonian Spit and their evolution. The evolution of the same switching type is represented by a horizontal sequence of images.

1) *Erosion scenario (E)*. The shoreline retreated throughout the entire sandbar switching zone. The E scenario was observed in 15 sandbar switching zones where shoreline retreat zone was between 285 and 1258 m in length (646 on average). The average shoreline retreat area for the E scenario was 15.5 m^2/m.
2) *Accretion-erosion-accretion scenario (A-E-A)*. The shoreline retreated in the middle part of the sandbar switching zone and advanced or remained stable in the northern and southern parts of the switching zone. The A-E-A scenario was observed in 6 sandbar switching zones where the middle shoreline retreat zone was between 196 and 696 m in length (343 m on average), and the sum length of the outer shoreline advance zones was between 233 and 944 m (546 on average). The average shoreline retreat and shoreline advance areas were 6.7 m^2/m and 17.8 m^2/m, respectively.
3) *Accretion-erosion scenario (A-E)*. The shoreline retreated in the northern or southern parts of the sandbar switching zone and advanced or remained stable in the remaining part. The A-E scenario was observed in 2 sandbar switching zones where the shoreline retreat and advance zones were equal to 443 and 233 m in length on average. The average shoreline retreat and advance areas were 16 and 9.5 m^2/m, respectively.
4) *Erosion-accretion-erosion scenario (E-A-E)*. The shoreline retreated in a major part of the sandbar switching zone with a small middle section remaining stable or advancing. The E-A-E scenario was observed in 2 sandbar switching zones where the outer retreat zones and mid-

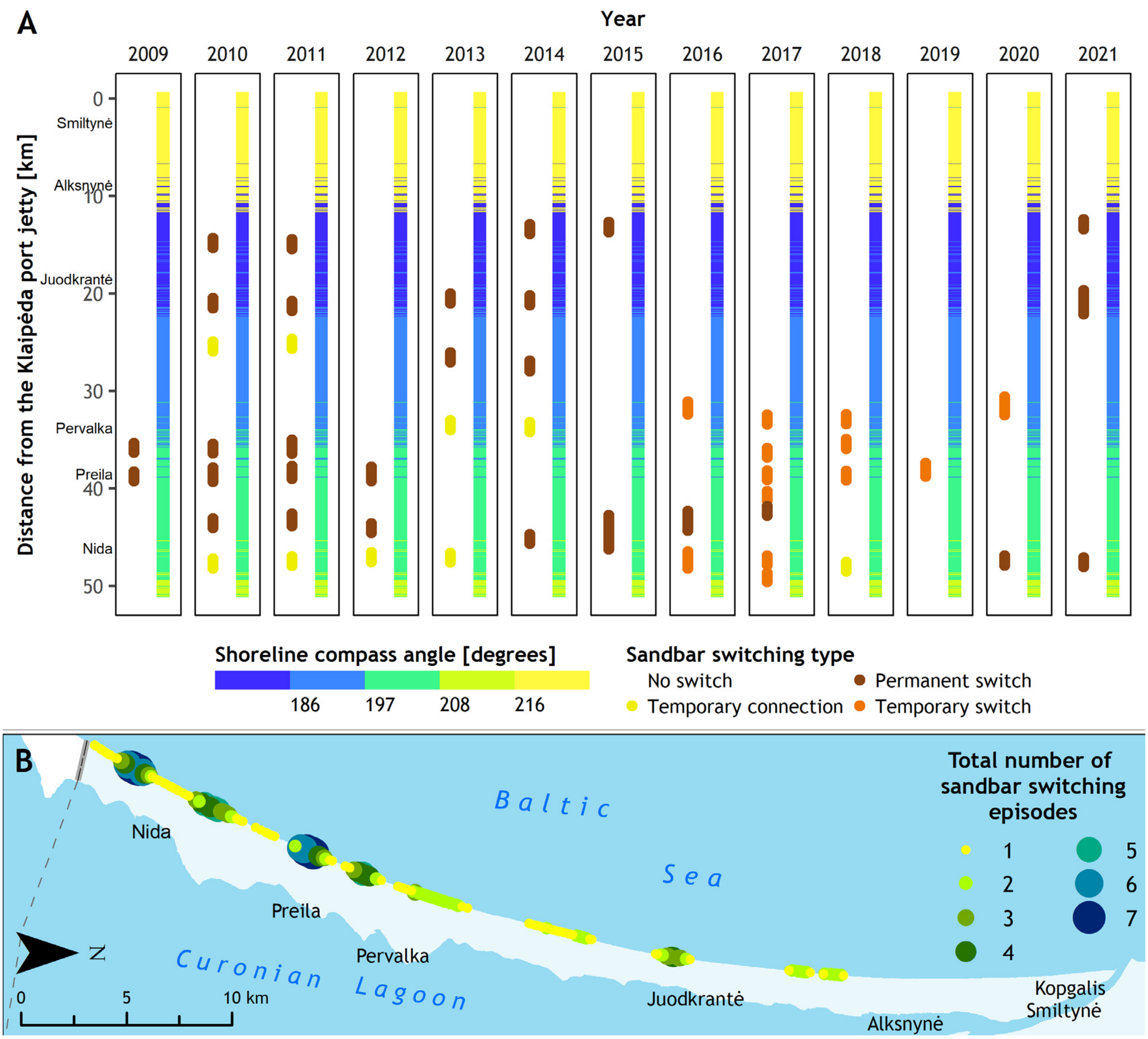

Figure 4 Spatial distribution of the sandbar switching zones on the Curonian Spit in 2009—2021: A — shoreline orientation and locations of sandbar switching zones by year. The sandbar switches tended to occur at the breaking points of different shoreline orientations. The shoreline orientation was calculated as a compass angle of mean shoreline position, which was divided into equal transects with a spacing of 25 m. B — spatial distribution of the total reoccurrence of sandbar switching episodes.

dle advance zone were 612 and 115 m in length on average, respectively. The average shoreline retreat area was 8.2 m^2/m, and the average shoreline advance area was 6.6 m^2/m.

3.3. Sand volume changes in the sandbar switching zones

3.3.1. Interannual sand volume change

During the period 2009—2021, 319 topographic cross-shore profiles were measured, with 30 in the sandbar switching zones. The average sand volume change in the beach-foredune system was 3.2 m^3/m (0.6%) and -3.5 m^3/m (-0.8%) at profiles outside and within the sandbar switching zones, respectively (Figure 6). According to the t-test results, the averages of the cubic sand volume change at profiles with and without sandbar switches were significantly different with 95% confidence ($p<0.05$) (Figure 6b). However, the averages of the percentage sand volume change in the beach-foredune system at profiles with and without sandbar switches were strongly influenced by the outliers, and an average comparison resulted in no significant results (Figure 6). To overcome the influence of the outliers, the medians of the interannual sand volume change were compared using a Wilcoxon test. Both the median of the percentage sand volume change and the median of the cubic sand volume change, at profiles with and without sandbar switches, were significantly different with 95% confidence ($p<0.05$) (Figure 6). The significantly different average and median rates of sand volume change at locations within and outside sandbar switching zones suggest that the sandbar switching was related to higher coastal erosion rates than

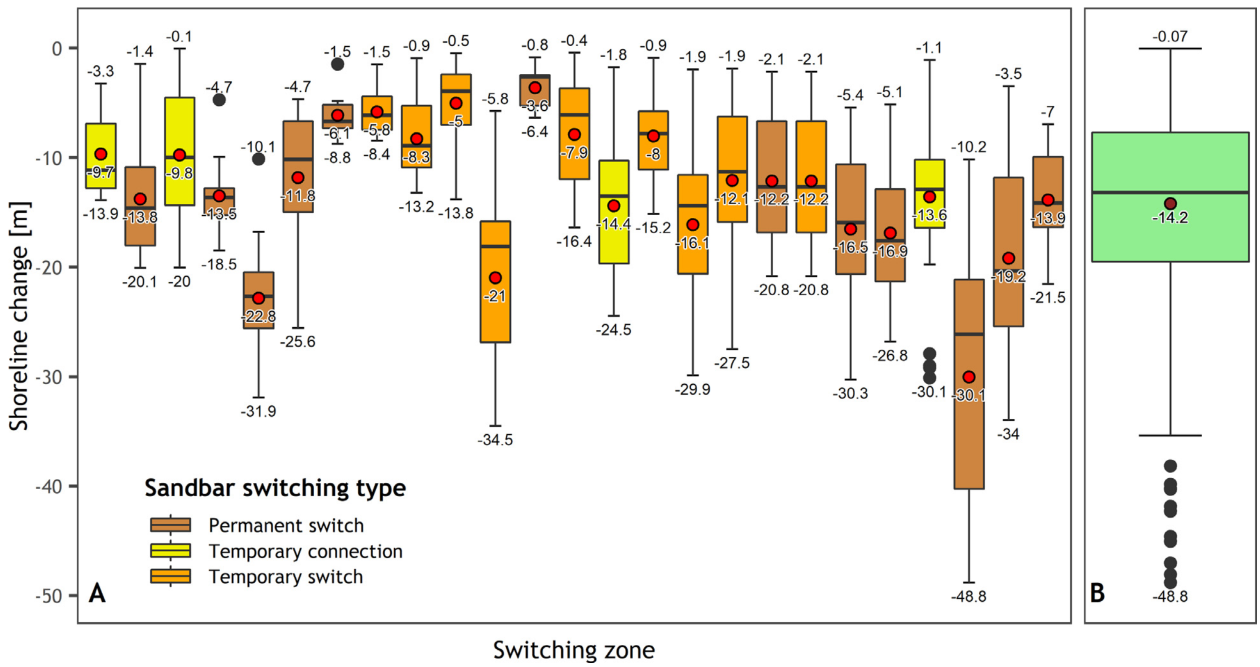

Figure 5 Boxplots defining the shoreline retreat characteristics within each sandbar switching zone in order of switching occurrence (from the earliest (left) to the latest (right)) (A) and combined for all the switching zones (B). The shoreline retreat characteristics were assessed for the transects located within the shoreline retreat area with 25 m spacing on the date of maximum shoreline retreat.

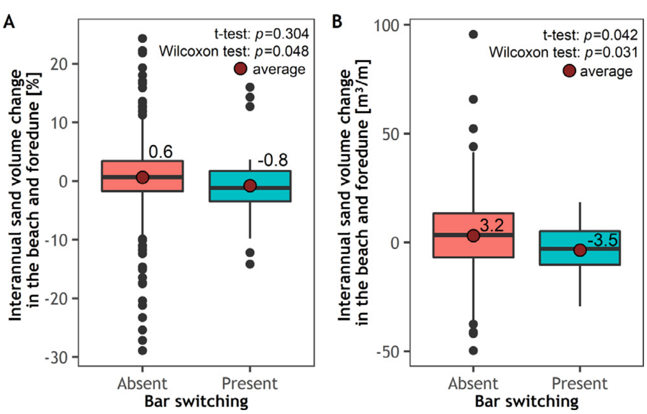

Figure 6 Comparison of the sand volume changes in the coastal cross-shore profiles when sandbar switching was absent or present. A — percentage of sand volume change; B — sand volume change in m^3/m.

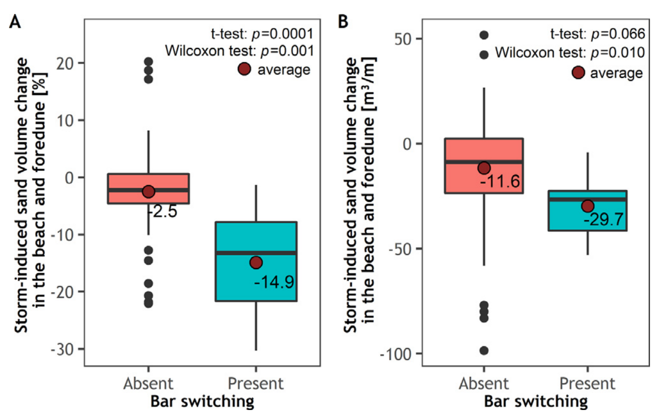

Figure 7 Comparison of the sand volume changes in the coastal cross-shore profiles during major storms when sandbar switching was absent or present. A — percentage of sand volume change; B — sand volume change in m^3/m.

locations outside the switching zones where accretion and dynamic equilibrium are dominant.

3.3.2. Sand volume change during major storms

During the last two decades, four major storms with wind speed exceeding the hurricane-force threshold ($\geq$ 32.6 m/s) have hit the coast of the Curonian Spit: Anatol in 1999, Erwin in 2005, Felix in 2015, and Laura in 2020. The main characteristics of winds, water levels, and changes in sand volume during the most destructive storms are summarised in Table 2. Only storms Anatol, Felix, and Laura were considered in this study because, during storm Erwin, the coast of the Curonian Spit gained 3.3 m^3/m of sand due to the high sediment supply from the southern part of the Curonian Spit (Kaliningrad oblast) and no considerable damage was done.

Eight sandbar switching episodes were observed at the locations of the topographic cross-shore profiles before major storm events (2 before Anatol, 3 before Felix, and 3 before Laura). The average rate of sand volume change in the beach-foredune system after major storm events was −11.6 m^3/m (−2.5%) and −29.7 m^3/m (−14.9%) at profiles outside and within the sandbar switching zones, respectively (Figure 7). According to the t-test results, the averages of the cubic sand volume change at profiles with and without switches were not significantly different (p=0.066)

Table 2 The main characteristics of major storms on the Curonian Spit.

Storm	Date	Mean maximal wind speed [m/s]	Gust wind speed [m/s]	Prevailing wind direction	Water level [m]	Sand volume change [m^3/m]
Anatol	4 December 1999	25	45.0	SW—SWS	+1.65	-35.7
Erwin	8—9 January 2005	25	33.0	W—WSW	+1.54	+3.3
Felix	11 January 2015	25	32.6	WSW	+1.37	-7.7
Laura	12 March 2020	28	36.4	W	+1.73	-2.0

(Figure 7b). One reason for this is that the result was influenced by sediment availability. The highest rate of erosion during the storm events was observed at profiles in the northern part of the study area with the largest sediment budget and where no sandbar switching was typically observed (Figure 4). For this reason, the percentage average sand volume changes were compared. The percentage averages of the sand volume change at profiles with and without switches were significantly different, with 95% confidence ($p<0.05$) (Figure 7a). According to a Wilcoxon test, the medians of the sand volume change were significantly different with 95% confidence ($p<0.05$) in both cases (percentage and cubic) (Figure 7).

3.4. Case studies of different coastal change scenarios

3.4.1. A case of erosion during a calm period

In this case, a sandbar switching episode occurred between 28 May 2008 and 2 August 2012 at the Preila rescue station. Multiple switches were observed in this sandbar switching zone. The episode occurred when the distance from the shoreline of the outer sandbar became discontinuous alongshore (Figure 8a). In 2009, the outer sandbar joined the middle sandbar, and the middle sandbar joined the inner sandbar. In 2010—2012, the outer sandbar join migrated north and the northern segment of the disconnected outer sandbar migrated south, while the distance between them decreased. In 2013, the discontinuous ends of the outer sandbar merged and continuity was restored in the sandbar system.

Two cross-shore profiles of interannual topographic surveys are located in this switching episode zone (Figure 8a). The coastal evolution in these profiles largely coincided with the evolution of switching episodes. Before the switching episode, the beach and foredune at profile 1 exhibited stability, then during the period 2008—2012, the beach and foredune experienced severe erosion with a sediment loss of 30—40 m^3/m per year (Figure 8c). After continuity was restored in the sandbar system, the accretion on the beach and foredune set in with a sediment gain of up to 20 m^3/m per year. Since 2016, coastal development has stabilised and dynamic equilibrium has set in. During the period of coastal instability (2009—2016), the correlation coefficient R between the sand volume change in the beach and foredune and the change in the distance from the shoreline of the outer sandbar was 0.78 ($p<0.05$). The switching location migrated north towards profile 2 (Figure 8b) and erosion at this profile started a year later with a sediment loss of 15—25 m^3/m per year (Figure 8d). In 2013, accretion processes began at a rate of 10—20 m^3/m per year. A period of large amount of accretion continued until 2016, when the development of the beach and foredune stabilised. During the period of coastal instability, correlation coefficient R between the sand volume change in the beach and foredune and the change in the distance from the shoreline of the outer sandbar was 0.48 ($p<0.05$). Changes in the shoreline and outer sandbar positions were in close agreement at profile 2 during the switching episode (R=0.85, $p<0.05$) (Figure 8f).

3.4.2. A case of erosion-accretion-erosion during a calm period

In this case, the switching episode occurred between 18 April 2019 and 5 October 2019. Temporary switches between outer-middle and middle-inner sandbars were observed when the outer and middle sandbars became discontinuous longshore and joined landward located sandbars. One cross-shore profile of interannual topographic surveys is located within this sandbar switching zone (Figure 9, profile 5). In 2018—2019, the year when a sandbar switching zone formation occurred, and in 2019—2020, the year when a sandbar switching episode occurred, the sand volume in the beach-foredune system for this profile decreased by over 20 m^3/m/y. In 2020—2021, the year after the sandbar switching episode ended, profile 5 gained 29.1 m^3/m of sand (Figure 9e).

The shoreline change within this sandbar switching zone was variable: the northern (profile 3) and southern parts (profile 5) of the switching zone suffered from shoreline retreat, and the middle part of 124 m (profile 4) underwent shoreline advance (Figure 9). On the date of maximum shoreline retreat, the area of shoreline erosion was 11.1 m^2/m with maximum and average shoreline retreat rates of 27.5 and 13.01 m, respectively. At profile 5, a decrease in the outer sandbar distance from the shoreline was followed by the highest shoreline recession within the switching zone (Figure 9d). The outer sandbar position at profiles 3 and 4 was quasi-stable during the switching episode, but at profile 3 the shoreline retreated, while at profile 4 the shoreline advanced at a rate of up to 12 m (Figure 9b,c). After the sandbar switching episode, the shoreline at profiles 3 and 5 started to recover. Correlation coefficient R between the shoreline change and the change in the outer sandbar distance from the shoreline in this zone was 0.59 ($p<0.05$) (Figure 9f).

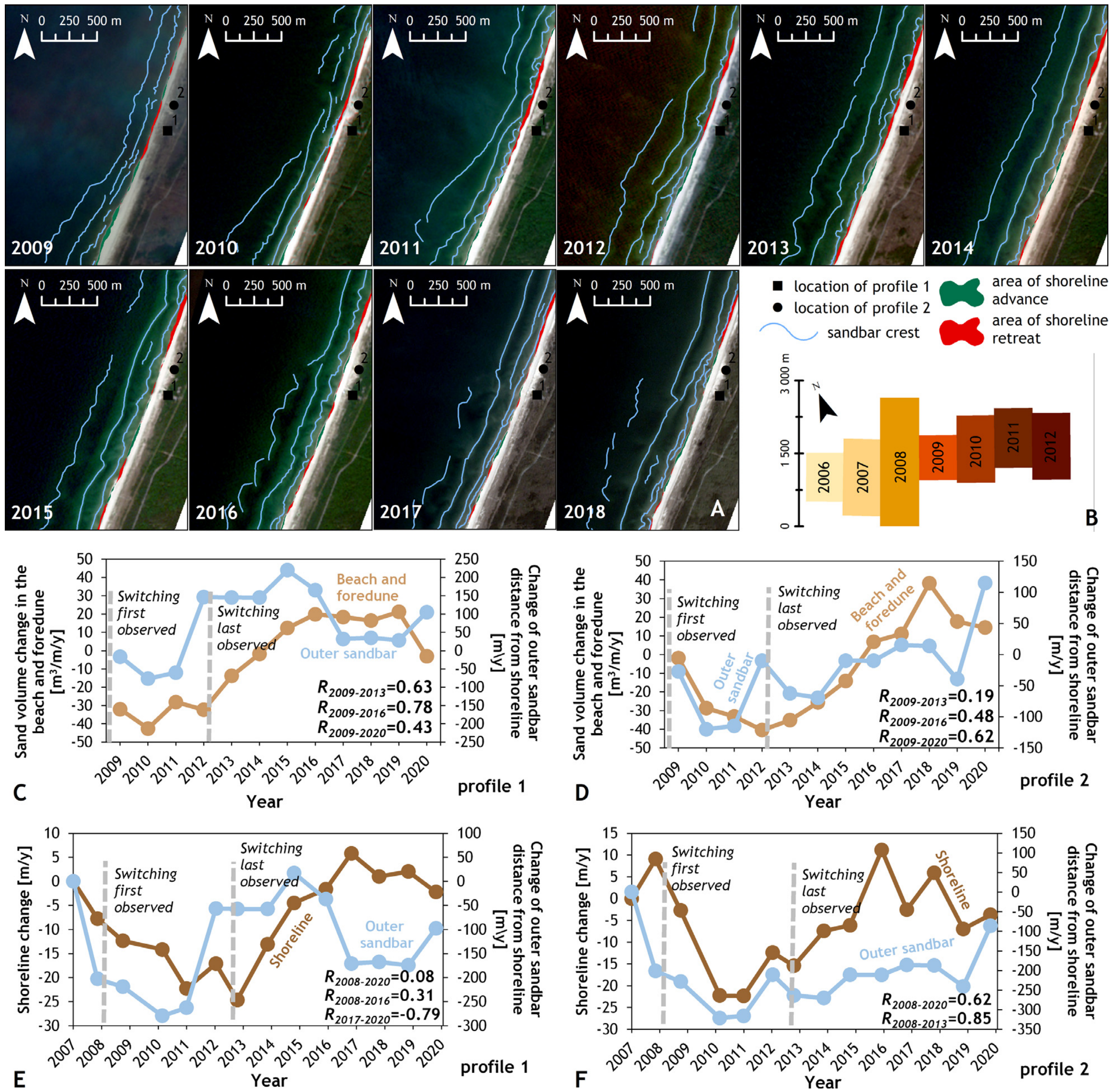

Figure 8 The coastal development during the sandbar switching episode at Preila: A — changes in the sandbar position; B — migration and length change of a sandbar switching zone; C, D — changes in the beach and foredune volume and outer sandbar distance from the shoreline at profiles 1 and 2; E, F — shoreline changes and change in the outer sandbar distance from the shoreline at profiles 1 and 2.

3.4.3. A case of erosion with storm influence

In this case, a sandbar switching episode occurred between 6 September 2014 and 6 October 2015. Here, a full switch between the outer and middle sandbars was observed. The switching episode occurred when the outer sandbar was split, and the northern segment of the disconnected outer sandbar joined the middle sandbar. During the switching episode, the southern end of the disconnected outer sandbar slowly decayed (Figure 10a).

During the switching episode, the Curonian Spit coast was hit by storm Felix (11 January 2015); therefore, this case represents switching-related coastal changes during storm events. In this case, two adjacent cross-shore profiles are analysed (profiles 6 and 7) (Figure 10). Both profiles experienced highly contrasting storm-induced changes. Profile 6, which was within the sandbar switching zone during storm Felix, lost 28.6 m^3/m of sand. Profile 7, which was outside the sandbar switching zone during storm Felix, gained 51.7 m^3/m of sand. During the overall period affected by the sandbar switching episode (2014—2016), profile 6 lost 51.1 m^3/m of sand while profile 7 gained 55.3 m^3/m. Almost identical rates of coastal erosion and accretion at profiles 6 and 7 suggest that the eroded sand within the sandbar switching zone was redistributed outside it, around the location of profile 7. The sand volume change within this switching zone was well correlated with

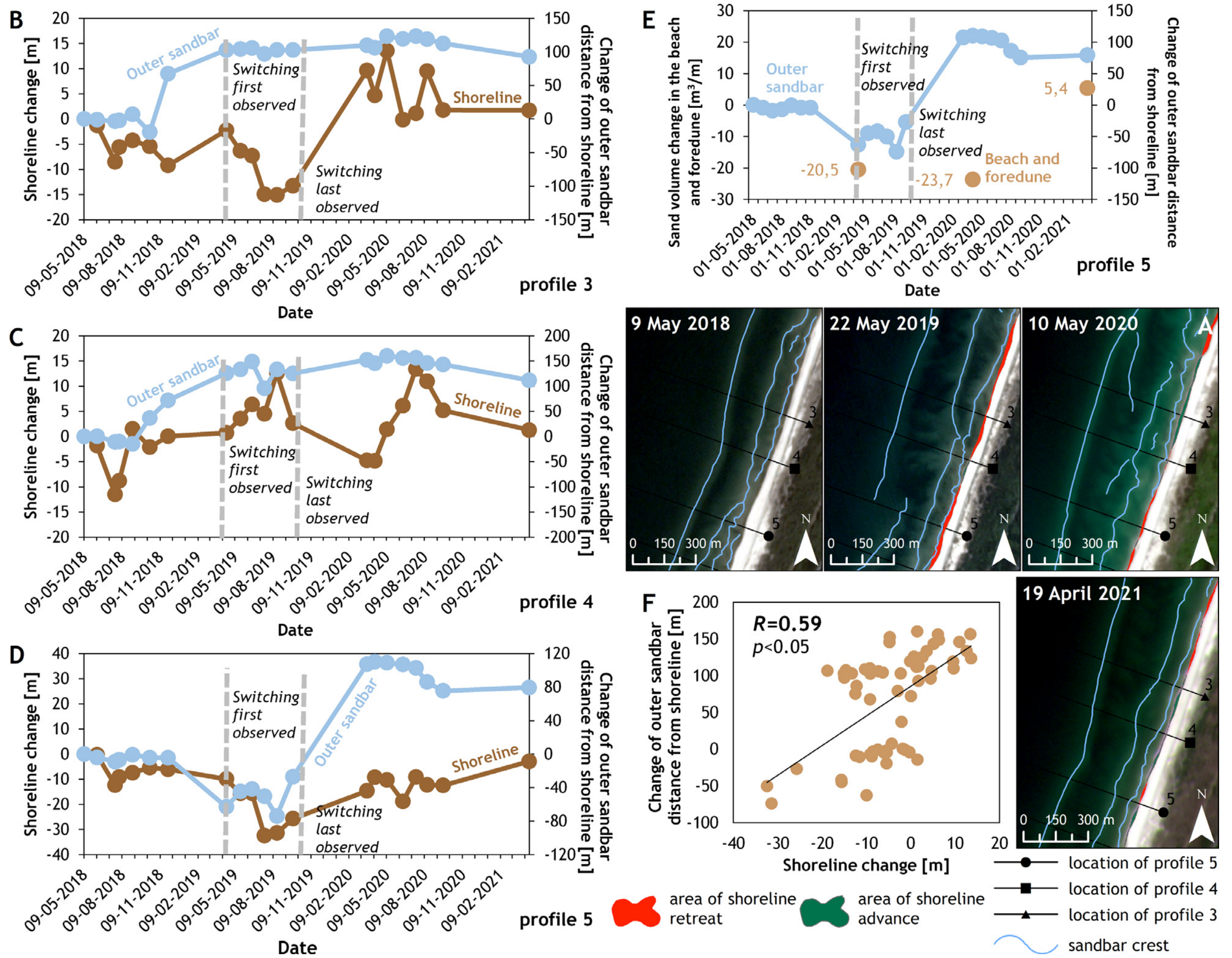

Figure 9 The coastal development during one of the sandbar switching episodes: A — changes in the sandbar position before, during, and after the switching episode; B — change of shoreline and outer sandbar position at profile 3; C — at profile 4, D — at profile 5; E — sand volume change in the beach-foredune system and outer sandbar position change at profile 5; F — the relationship between the changes in the shoreline and outer sandbar position at profiles 3, 4 and 5.

the switching-related changes of the outer sandbar cross-shore position (R=0.86, p<0.05) (Figure 10d). The shoreline position changes at profiles 6 and 7 were less consistent with the changes in the sandbar position (R=0.49, p<0.05) (Figure 10d).

4. Discussion

In this study, the sandbar switching phenomenon in multiple sandbar systems and its relation to beach-foredune system changes are analysed by using decadal data from satellite imagery and topographic surveys. On the Curonian Spit, sandbar switching episodes are observed from 13 km from the Klaipėda port jetty and further to the south in quasi-stable locations (in most cases) where they tend to reoccur multiple times. A set of specific hydrodynamic conditions and specific antecedent morphology (discontinuity in longshore sandbar development) is necessary for the formation of sandbar switches (Shand et al., 2001; Walstra et al., 2016; Wijnberg and Wolf, 1994). Due to the north-eastern coastal orientation and the predominant south-westerly wind and wave direction (Jakimavičius et al., 2018), cross-shore sediment transport is dominant in the northern part of the Curonian Spit (Žilinskas et al., 2018), resulting in no observed sandbar switches; with the changing shoreline orientation to northern-southern and south-western, the longshore currents become stronger and the longshore sediment transport prevails where sandbar switches are typically observed. This result is consistent with previous studies suggesting that switching formation requires obliquely incident wave events and strong longshore currents (Aleman et al., 2017; Shand et al., 2001).

Apart from the oblique waves and strong longshore currents, the main cause of sandbar switching formation is an alongshore discontinuity in the sandbar system development (Aleman et al., 2017; Shand et al., 2001; Walstra et al., 2016) which is determined by alongshore differences in the hydrodynamic and morphodynamic conditions. Therefore, the ideal conditions for sandbar switching to occur would be transitional zones where different hydrodynamic and morphodynamic conditions collide. Differences in shoreline

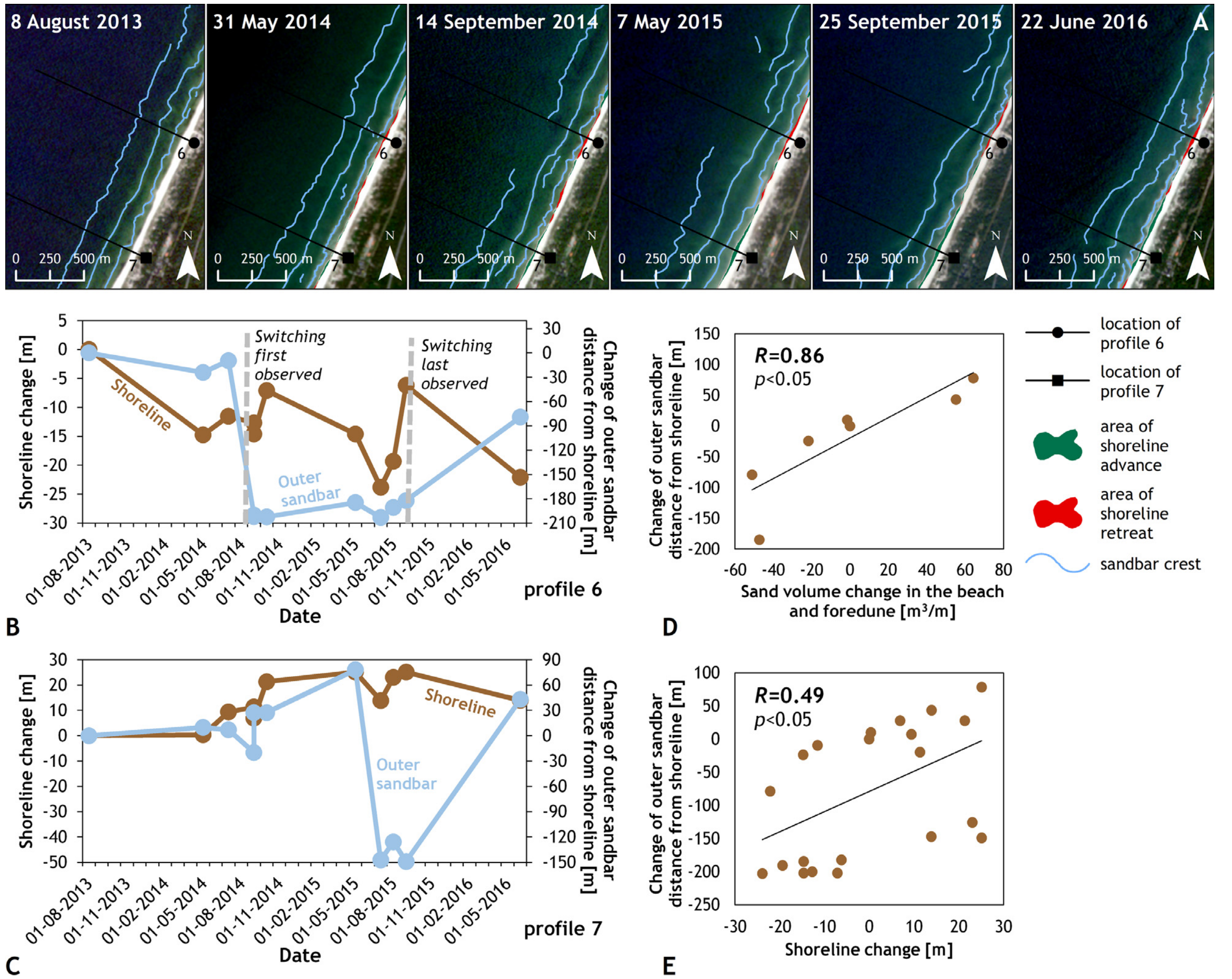

Figure 10 The coastal development during sandbar switching episode and storm Felix (profile 6 represents development within the switching zone; profile 7 — outside the switching zone): A — changes in the sandbar position; B — changes in the shoreline and outer sandbar position at profile 6; C — changes in the shoreline and outer sandbar position at profile 7; D — relationship between the changes in sand volume on the beach and foredune, and changes in the outer sandbar position at profiles 6 and 7; E — relationship between the changes in the shoreline and outer sandbar positions at profiles 6 and 7.

orientation are one of the factors causing the formation of such transitional zones. The results of this study demonstrate that transitional zones between predominant shoreline compass angle coincide with typical locations of sandbar switching formation (Figure 4a).

On the basis of the above described, the essential conditions for the occurrence of sandbar switching episodes would be locations where the breakpoint of different shoreline orientations and shore-oblique waves with associated longshore currents coincide. The described complex of conditions could be used to identify potential locations where sandbar switches occur. In Figure 11, the shoreline compass angle and averaged deviation of wave propagation angle from the shore-normal angle, calculated for longshore stretches of 1 km for the period between 2009 and 2020, are used as the independent variables in the logistic regression model for the prediction of sandbar switching locations. Using both metrics, a sandbar switching location can be predicted with McFadden's pseudo R^2 of 0.57. However, using the deviation of wave direction only, R^2 is 0.54. This suggests that the contribution of shoreline direction to the accuracy of the model is minor, and the direction of wave propagation is more important for the prediction of sandbar switching formation.

Although it has been almost three decades since the longshore realignment of nearshore sandbars was observed and identified for the first time (Shand et al., 2001; Wijnberg and Wolf, 1994), the way this phenomenon affects the development of subaerial beaches has never been studied before. In this study, the emergence of coastal erosion within sandbar switching zones, including a decrease in sand volume in a beach-foredune system and shoreline retreat on interannual and storm-related time scales, was observed for the first time. This shows that the longshore realignment of nearshore sandbars plays an important role in the development of a beach-foredune system. The causes of this connection could be twofold: 1) switching-related changes in sandbar morphology affect the overall nearshore flow field

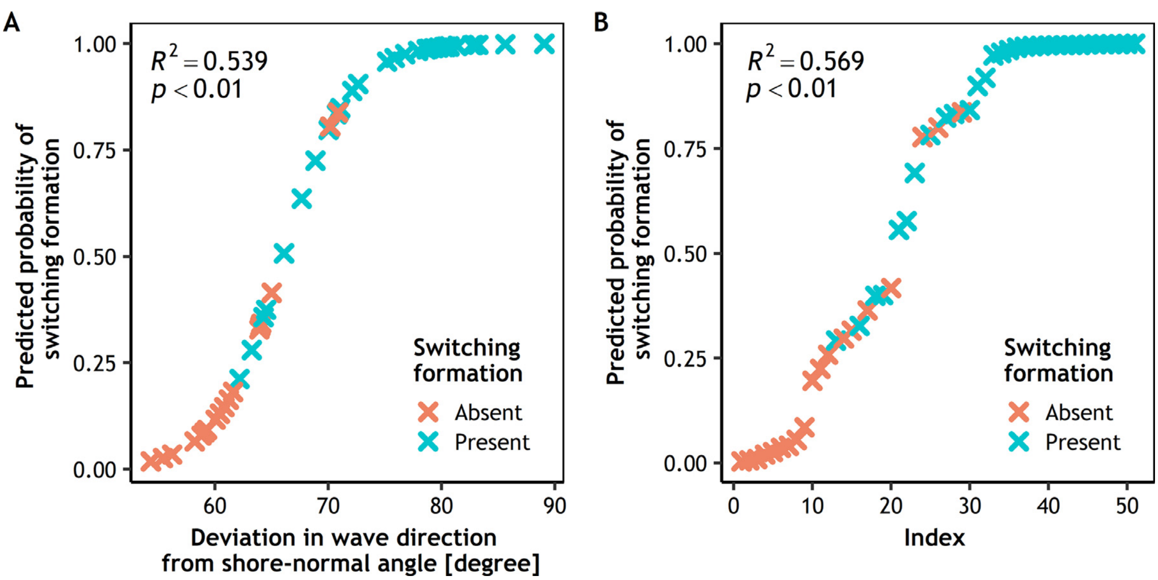

Figure 11 Logistic regression model for the sandbar switching formation: A — model with a deviation in wave direction from a shore-normal angle as the independent variable; B — model with a change in the shoreline compass angle and deviation in wave direction from a shore-normal angle as independent variables. The colour in the figure indicates the observed values (true) and the point locations indicate the predicted probability of sandbar switching formation. The R^2 value was calculated as McFadden-pseudo-R-squared.

and disturb the usual sediment exchange between the beach and nearshore; 2) sandbar switching zones are often related to the local diminishing in width of the nearshore sandbar zone (e.g., when the outer sandbar splits and connects to the landward sandbar). Nearshore sandbars act as natural barriers, dissipating wave energy (Dubarbier et al., 2015; Fernández-Mora et al., 2015; Plant et al., 2001; Price et al., 2014); when this barrier disappears or the sandbar zone diminishes, the portion of dissipated wave energy decreases and the portion of wave energy which reaches the coastline increases near the location of the diminished sandbar zone, thus causing increased rates of local coastal erosion. This assumption is based on case studies of sandbar switching zones, showing strong and moderate agreement between changes in shoreline position, changes in sand volume in the beach-foredune system, and changes in the outer sandbar position during sandbar switching episodes. Additional observations on other non-tidal and microtidal sandy beaches with multiple sandbar systems, exhibiting patterns of sandbar realignment, could confirm the relation between the sandbar switching episodes and coastal erosion observed along the Curonian Spit coast and should seek to identify the exact causes of this connection.

5. Conclusions

The present study analyses the switching-related morphodynamic behaviour of multiple sandbar system and its connection to changes in a shoreline and beach-foredune system on the Curonian Spit, located along the South-Eastern Baltic Sea coast. It is determined that sandbar switches on the Curonian Spit prefer quasi-stable locations where sandbar switching episodes are repeatedly observed. These preferred locations coincide with transitional zones between different prevailing shoreline compass angles and oblique wave energy. Typical sandbar switching episode lasts for over a year or longer and affect the nearshore flow field from seasonal to interannual time scales.

The emergence of coastal erosion processes within sandbar switching zones was observed in this study. On an interannual time scale, the beach and foredune experienced a small average rate of erosion during the sandbar switching episodes compared to locations outside the sandbar switching zones, which exhibit a small average rate of accretion. On a storm-related time scale, a higher average rate of beach and foredune erosion was observed within the sandbar switching zones than at locations outside those zones. During the switching episodes, the shoreline typically retreats landward and recovers after a sandbar switching episode. It is hypothesised that increased coastal erosion at switching locations could be related to an imbalance in the typical sediment exchange between the beach and nearshore, and a local diminishing of the sandbar zone both caused by sandbar switching-induced changes in the nearshore morphology and nearshore flow field. This assumption is partly confirmed by case studies of coastal development within sandbar switching zones, demonstrating that the position of the outer sandbar is well correlated with the shoreline and beach-foredune volume changes during sandbar switching episodes: when the distance from the shoreline of the outer sandbar decreases, the beach dynamic state moves towards erosion. The relationship between sandbar switching and coastal erosion has been observed and assessed for the first time, no previous studies analysing the morphodynamic connection between sandbar switching zones and subaerial domain exist. Therefore, further studies should seek to confirm this relationship and identify the processes behind it.

The results of this study reveal the importance of the sandbar switching phenomenon in coastal development and suggest that the identification of potential sandbar switching locations could be used to find potential coastal erosion hot spots. Also, the study results imply that sandbar switching zones are characterised by a high variability of coastal changes. This observation could be important for coastal prediction.

Declaration of competing interest

The authors declare that they have no known competing financial interests or personal relationships that could have appeared to influence the work reported in this paper.

Acknowledgments

This research did not receive any specific grant from funding agencies in the public, commercial, or non-profit sectors. The authors wish to thank Viktoras Karaliūnas (Nature Research Centre, Lithuania) for the technical support and two anonymous reviewers for their useful suggestions.

References

Aagaard, T., Davidson-Arnott, R., Greenwood, B., Nielsen, J., 2004. Sediment supply from shoreface to dunes: Linking sediment transport measurements and long-term morphological evolution. Geomorphology 60, 205—224. https://doi.org/10.1016/j.geomorph.2003.08.002

Aleman, N., Certain, R., Robin, N., Barusseau, J.P., 2017. Morphodynamics of slightly oblique nearshore bars and their relationship with the cycle of net offshore migration. Mar. Geol. 392, 41—52. https://doi.org/10.1016/j.margeo.2017.08.014

Balouin, Y., Tesson, J., Gervais, M., 2013. Cuspate shoreline relationship with nearshore bar dynamics during storm events — field observations at Sete beach, France. J. Coast. Res. 65, 440—445. https://doi.org/10.2112/SI65-075.1

Bouvier, C., Balouin, Y., Castelle, B., 2017. Video monitoring of sandbar-shoreline response to an offshore submerged structure at a microtidal beach. Geomorphology 295, 297—305. https://doi.org/10.1016/j.geomorph.2017.07.017

Brooks, S.M., Spencer, T., Christie, E.K., 2017. Storm impacts and shoreline recovery: Mechanisms and controls in the southern North Sea. Geomorphology 283, 48—60. https://doi.org/10.1016/j.geomorph.2017.01.007

Castelle, B., Marieu, V., Bujan, S., Bujan Alongshore-Variable Beach, S., Changes, D., 2019. Alongshore-Variable Beach and Dune Changes on the Timescales from Days (Storms) to Decades Along the Rip-dominated Beaches of the Gironde Coast, SW France. J. Coast. Res. SI 88, 157—171. https://doi.org/10.2112/SI88-012.1

Castelle, B., Marieu, V., Bujan, S., Splinter, K.D., Robinet, A., Sénéchal, N., Ferreira, S., 2015. Impact of the winter 2013-2014 series of severe Western Europe storms on a double-barred sandy coast: Beach and dune erosion and megacusp embayments. Geomorphology 238, 135—148. https://doi.org/10.1016/j.geomorph.2015.03.006

Castelle, B., Turner, I.L., Ruessink, B.G., Tomlinson, R.B., 2007. Impact of storms on beach erosion: Broadbeach (Gold Coast, Australia). J. Coast. Res. 50, 534—539.

Cohn, N., Ruggiero, P., De Vries, S., García-Medina, G., 2017. Beach growth driven by intertidal sandbar welding. In: Coastal Dynamics, Helsingør, 2017, 12—16.

Del Río, L., Gracia, F.J., Benavente, J., 2013. Shoreline change patterns in sandy coasts. A case study in SW Spain. Geomorphology 196, 252—266. https://doi.org/10.1016/j.geomorph.2012.07.027

Dubarbier, B., Castelle, B., Marieu, V., Ruessink, G., 2015. Process-based modeling of cross-shore sandbar behavior. Coast. Eng. 95, 35—50. https://doi.org/10.1016/j.coastaleng.2014.09.004

Fernández-Mora, A., Calvete, D., Falqués, A., De Swart, H.E., 2015. Onshore sandbar migration in the surf zone: New insights into the wave-induced sediment transport mechanisms. Geophys. Res. Lett. 42, 2869—2877. https://doi.org/10.1002/2014GL063004

Gijsman, R., Ruessink, B.G., Visscher, J., Schlurmann, T., 2021. Observations on decadal sandbar behaviour along a large-scale curved shoreline. Earth Surf. Process. Landforms 46, 490—503. https://doi.org/10.1002/esp.5041

Harley, M.D., Turner, I.L., Short, A.D., Ranasinghe, R., 2009. An empirical model of beach response to storms-SE Australia. In: 19th Australasian Coastal and Ocean Engineering Conference 2009 and the 12th Australasian Port and Harbour Conference 2009, Coasts and Ports, 2009, 589—595.

Jakimavičius, D., Kriaučiūnienė, J., Šarauskienė, D., 2018. Assessment of wave climate and energy resources in the Baltic Sea nearshore (Lithuanian territorial water). Oceanologia 60 (2), 207—218. https://doi.org/10.1016/j.oceano.2017.10.004

Janušaitė, R., Jukna, L., Jarmalavičius, D., Pupienis, D., Žilinskas, G., 2021. A Novel GIS-Based Approach for Automated Detection of Nearshore Sandbar Morphological Characteristics in Optical Satellite Imagery. Remote Sens. 13, 2233. https://doi.org/10.3390/rs13112233

Jarmalavičius, D., Žilinskas, G., Pupienis, D., 2017. Geologic framework as a factor controlling coastal morphometry and dynamics. Curonian Spit, Lithuania. Int. J. Sediment Res. 32, 597—603. https://doi.org/10.1016/j.ijsrc.2017.07.006

Kelpšaitė, L., Dailidienė, I., 2011. Influence of wind wave climate change on coastal processes in the eastern Baltic Sea. J. Coast. Res. 64, 220—224.

Kuznetsova, O., Saprykina, Y., 2019. Influence of Underwater Bar Location on Cross-Shore Sediment Transport in the Coastal Zone. J. Mar. Sci. Eng. 7, 55. https://doi.org/10.3390/jmse7030055

McFeeters, S.K., 1996. The use of the Normalized Difference Water Index (NDWI) in the delineation of open water features. Int. J. Remote Sens. 17, 1425—1432. https://doi.org/10.1080/01431169608948714

McNinch, J.E., 2004. Geologic control in the nearshore: Shore-oblique sandbars and shoreline erosional hotspots, Mid-Atlantic Bight, USA. Mar. Geol. https://doi.org/10.1016/j.margeo.2004.07.006

Ojeda, E., Ruessink, B.G., Guillen, J., 2008. Morphodynamic response of a two-barred beach to a shoreface nourishment. Coast. Eng. 55, 1185—1196. https://doi.org/10.1016/j.coastaleng.2008.05.006

Parlagreco, L., Melito, L., Devoti, S., Perugini, E., Soldini, L., Zitti, G., Brocchini, M., 2019. Monitoring for Coastal Resilience: Preliminary Data from Five Italian Sandy Beaches. Sensors 19, 1854. https://doi.org/10.3390/s19081854

Phillips, M.S., Harley, M.D., Turner, I.L., Splinter, K.D., Cox, R.J., 2017. Shoreline recovery on wave-dominated sandy coastlines: the role of sandbar morphodynamics and nearshore wave parameters. Mar. Geol. 385, 146—159. https://doi.org/10.1016/j.margeo.2017.01.005

Planet, 2021. Planet Imagery Products Specifications [WWW Document]. https://assets.planet.com/docs/Planet_Combined_Imagery_Product_Specs_letter_screen.pdf (accessed 5.9.21).

Planet Team, 2017. Planet Application Program Interface: In Space for Life on Earth [WWW Document]. https://api.planet.com/ (accessed 5.9.21).

Plant, N.G., Freilich, M.H., Holman, R.A., 2001. Role of morphologic feedback in surf zone sandbar response. J. Geophys. Res. Ocean. 106, 973—989. https://doi.org/10.1029/2000JC900144

Price, T.D., Ruessink, B.G., Castelle, B., 2014. Morphological coupling in multiple sandbar systems — A review. Earth Surf. Dyn. https://doi.org/10.5194/esurf-2-309-2014

Pruszak, Z., Różyński, G., Szmytkiewicz, P., 2008. Megascale rhythmic shoreline forms on a beach with multiple bars. Oceanologia 50 (2), 183—203.

Quartel, S., Kroon, A., Ruessink, B.G., 2008. Seasonal accretion and erosion patterns of a microtidal sandy beach. Mar. Geol. 250, 19—33. https://doi.org/10.1016/j.margeo.2007.11.003

Ruessink, B.G., Coco, G., Ranasinghe, R., Turner, I.L., 2007. Coupled and noncoupled behavior of three-dimensional morphological patterns in a double sandbar system. J. Geophys. Res. Ocean. 112. https://doi.org/10.1029/2006JC003799

Shand, R.D., 2003. Relationships between episodes of bar switching, cross-shore bar migration and outer bar degeneration at Wanganui, New Zealand. J. Coast. Res. 19, 157—170.

Shand, R.D., Bailey, D.G., 1999. A review of net offshore bar migration with photographic illustrations from Wanganui, New Zealand. J. Coast. Res. 15, 365—378.

Shand, R.D., Bailey, D.G., Shepherd, M.J., 2001. Longshore realignment of shore-parallel sand-bars at Wanganui, New Zealand. Mar. Geol. 179, 147—161. https://doi.org/10.1016/S0025-3227(01)00223-7

Shand, R.D., Hesp, P.A., Shepherd, M.J., 2006. Beach Cut In Relation To Net Offshore Bar Migration Characteristics of Beach Cut. J. Coast. Res. 2004, 334—340.

Splinter, K.D., Gonzalez, M.V.G., Oltman-Shay, J., Rutten, J., Holman, R., 2018. Observations and modelling of shoreline and multiple sandbar behaviour on a high-energy meso-tidal beach. Cont. Shelf Res. 159, 33—45. https://doi.org/10.1016/j.csr.2018.03.010

Stive, M.J.F., Aarninkhof, S.G.J., Hamm, L., Hanson, H., Larson, M., Wijnberg, K.M., Nicholls, R.J., Capobianco, M., 2002. Variability of shore and shoreline evolution. Coast. Eng. 47, 211—235. https://doi.org/10.1016/S0378-3839(02)00126-6

Stive, M.J.F., Guillen, J., Capobianco, M., 1997. Bar migration and duneface oscillation on decadal scales. In: Proceedings of the 25th Coastal Engineering Conference 1996, 2884—2896. https://doi.org/10.1061/9780784402429.223

Tătui, F., Vespremeanu-Stroe, A., Preoteasa, L., 2013. The correlated behavior of sandbars and foredunes on a nontidal coast (Danube Delta, Romania). J. Coast. Res. 5 (Sp. 2). https://doi.org/10.2112/si65-317.1

Thornton, E.B., MacMahan, J., Sallenger, A.H., 2007. Rip currents, mega-cusps, and eroding dunes. Mar. Geol. 240, 151—167. https://doi.org/10.1016/j.margeo.2007.02.018

Umeda, S., Yuhi, M., Karunarathna, H., 2018. Seasonal to Decadal Variability of Shoreline Position on a Multiple Sandbar Beach. J. Coast. Res. 85, 261—265. https://doi.org/10.2112/si85-053.1

USGS, 1998. USGS EROS Archive - Landsat Archives - Landsat 4-5 Thematic Mapper (TM) Level-1 Data Products. https://doi.org/10.5066/P9IAXOVV

Van de Lageweg, W.I., Bryan, K.R., Coco, G., Ruessink, B.G., 2013. Observations of shoreline-sandbar coupling on an embayed beach. Mar. Geol. 344, 101—114. https://doi.org/10.1016/j.margeo.2013.07.018

Vermaas, T., Elias, E., Van Der Spek, A., Hoogland, R., 2017. Time-dependent effects of nourishments on shoreface bar behaviour. In: Coastal Dynamics, Helsingør, 2017, 862—869.

Walstra, D.-J., Wesselman, D., van der Deijl, E., Ruessink, G., 2016. On the Intersite Variability in Inter-Annual Nearshore Sandbar Cycles. J. Mar. Sci. Eng. 4, 15. https://doi.org/10.3390/jmse4010015

Wijnberg, K.M., Aarninkhof, S.G.J., Spanhoff, R., 2007. Response of a shoreline sand wave to beach nourishment. In: Proceedings of the 30th Coastal Engineering Conference 2006. World Scientific Publishing Company, 4205—4217. https://doi.org/10.1142/9789812709554_0353

Wijnberg, K.M., Wolf, F.C.J., 1994. Three-dimensional behaviour of a multiple bar system. In: Proceedings of Coastal Dynamics'94. ASCE, 59—73.

Yuhi, M., Matsuyama, M., Hayakawa, K., 2016. Sandbar Migration and Shoreline Change on the Chirihama Coast, Japan. J. Mar. Sci. Eng. 4, 40. https://doi.org/10.3390/jmse4020040

Yuhi, M., Umeda, S., 2018. Characteristics of Systematic Migrations of Multiple Sandbars and Related Cross-Shore Sediment Transport at Chirihama and Adjacent Coasts, Japan. J. Coast. Res. 85, 231—235. https://doi.org/10.2112/si85-047.1

Žilinskas, G., Janušaitė, R., Jarmalavičius, D., Pupienis, D., 2020. The impact of Klaipėda Port entrance channel dredging on the dynamics of coastal zone, Lithuania. Oceanologia 62 (4PA), 489—500. https://doi.org/10.1016/j.oceano.2020.08.002

Žilinskas, G., Jarmalavičius, D., Pupienis, D., 2018. The influence of natural and anthropogenic factors on grain size distribution along the southeastern Baltic spits. Geol. Q. 62, 375—384. https://doi.org/10.7306/gq.1413